Journal of Food Measurement and Characterization
https://doi.org/10.1007/s11694-025-03168-y

ORIGINAL PAPER

A hand-like gripper embedded with flexible gel sensor for tomato harvesting: soft contact and intelligent ripeness sensing

Wangyu Liu[1] · **Zhenhua Tan**[1] · **Weigui Xie**[1,2]

Received: 13 June 2024 / Accepted: 18 February 2025

Abstract

With the continuous growth of tomato yields and the need to address the cumbersome task of manual harvesting, the development of harvesting robots presents a promising solution for tomato harvesting. A key challenge lies in improving the success rate of these robots for reliable tomato harvesting without causing damage. This study aims to propose a rigid-flexible coupled gripper to ensure higher success rates in tomato harvesting, while also incorporating an advanced method for detecting fruit ripeness. The paper introduces a flexible hydrogel pressure sensor, featuring a wide detection range, high sensitivity, and excellent stability, integrated into the gripper design. A signal acquisition system based on a sensor array is developed, enabling the accurate capture of force signals during the tomato grasping process. The sensor array collects tactile sequence data in real-time, which, when combined with compressive deformation data from the fruit, forms a comprehensive dataset. To detect tomato ripeness, four classification models—Long Short-Term Memory (LSTM), Convolutional Neural Networks (CNN), Multi-Layer Perceptron (MLP), and Fully Convolutional Networks (FCN)—are implemented. Among the four models, the LSTM network achieves the highest classification performance. The overall recognition accuracy for tomatoes of different ripeness levels, within the same variety and at room temperature, is determined to be 99%. The results demonstrate that the combination of a flexible gripper with hydrogel sensors not only preserves the integrity of the tomatoes but also ensures accurate detection of fruit ripeness. This innovation has the potential to significantly enhance the performance of tomato harvesting robots, contributing to more efficient and automated agricultural practices.

Keywords Harvesting gripper · Flexible sensor · Deep learning · Fruit ripeness

Introduction

Tomato is a crucial vegetable crop, with a global annual production exceeding 186 million tons [1]. Moreover, tomato and tomato-based products are important sources of many established nutrients and are predominant sources of some phytochemicals, which render many health benefits [2]. In the entire tomato production chain, the most time-consuming and labor-intensive process is harvesting [3], and consumers consistently seek tomatoes of high quality and optimal ripeness [4]. This hightlights the significance of both fruit harvesting quality and accurate ripeness determination in the automation of the tomato harvesting process. Not only does this alleviate the labor intensity in fruit storage and sorting procedures, but it also significantly enhances customer satisfaction and industry profit margins. The critical importance of automating the tomato harvesting process lies in meeting consumer preferences for tomatoes with excellent quality and optimal ripeness, thereby improving overall efficiency and economic viability in the tomato production industry. In recent years, with the advancements in machine vision technology and intelligent control techniques, the autonomous completion of tomato harvesting by intelligent robots has emerged as a new developmental trend [5–7]. The harvesting gripper, serving as the terminal component for interaction between the harvesting robot and tomatoes, significantly influences both the efficiency of harvesting operations and the damage rate of fruit. Consequently, the design of a gripper capable of facilitating damage-free tomato harvesting

✉ Weigui Xie
scutxwg@scut.edu.cn

[1] School of Mechanical and Automotive Engineering, South China University of Technology, Guangzhou City 510641, People's Republic of China

[2] School of Mechanical and Aerospace Engineering, Nanyang Technological University, 50 Nanyang Avenue, 639798 Singapore, Singapore

Published online: 03 March 2025

and discerning fruit ripeness during the harvesting process has become a critical challenge that urgently needs resolution in the field of tomato harvesting robotics. This emphasizes the pivotal role of the gripper in enhancing the overall performance and effectiveness of autonomous tomato harvesting systems.

Generally, grippers for harvesting robots can be categorized into three types: rigid grippers, flexible grippers, and rigid–flexible coupled grippers. Notably, rigid grippers have witnessed considerable advancements and achievements in the research and application of tomato harvesting. The team led by Chihsing Liu et al. [8] designed a dual-finger tomato gripper with sensory feedback, demonstrating adaptability in grasping tomatoes of various shapes. However, it lacks the control over gripping force, thereby compromising the assurance of damage-free harvesting. Takuya Fujinaga et al. [9] developed a rigid-tipped device for harvesting tomato clusters, which, although effective, is relatively cumbersome and achieves a harvesting success rate of 85%. While rigid grippers offer advantages such as stable gripping force, high precision, and high speed, their complex structure and insufficient flexibility may lead to damage to the fruit's skin, resulting in a lower success rate in harvesting. Conversely, flexible grippers exhibit continuous deformation when interacting with fruits, providing infinite degrees of freedom and significantly increasing structural flexibility. Hongyu Zhou et al. [10] proposed a flexible fruit harvesting device integrated with an array of tactile sensors. By analyzing sensor data during the harvesting process, it enables the detection of gripping slippage and thus enhances the precision of gripping force control. Fu Zhang et al. [11] investigated an end effector with human-like grasping capabilities, achieving a 95.82% success rate in harvesting cherry tomatoes, with an average harvesting time of 4.86 s and a harvesting damage rate of 2.90%. Currently, flexible grippers are more suitable for specific scenarios involving tomatoes. Rigid–flexible coupled grippers is an emerging research in agricultural harvesting, combining flexible and rigid structures to achieve more effective fruit harvesting. Jun Liu's [12] team designed a tomato gripper inspired by human harvesting behavior, exhibiting strong adaptability and stability. However, it lacked the ability to control harvesting force, leading to potential mechanical damage. Li Li's [13] team designed a rigid–flexible coupling three-finger soft gripper is present to grasp fruits. It can solve the problem that the traditional rigid manipulator is easy to damage the target object and the flexible manipulator has insufficient grasping force. Moreover, such a structure lacks force feedback, and the large size of the gripper makes it unsuitable for working in complex environments. The structural complexity of such end-effectors has not fully taken the advantages of both rigidity and flexibility, necessitating further in-depth research. In summary, there is currently limited integration of flexible sensors with harvesting robots to achieve flexible and safe harvesting. Moreover, intelligent assessment of physical properties such as ripeness during the harvesting process is rarely observed. Further investigation is imperative to optimize the design and functionality of such end effectors in the context of agricultural robotics.

According to the ripening process, tomato can be divided into immature stage, semi-mature stage and mature stage. In the immature stage, the fruit skin is pale green and white, the fruit surface is shiny, the accumulation of nutrients is basically complete, the content of aldehyde is high, and the flavor of grass is green, and the fruit is very hard. In the semi-mature stage, the skin gradually turns red, the content of volatile substances increases, the fruit taste is more obvious, the fruit gradually becomes soft, and it is not suitable for long-term storage. In the mature stage, the skin turns completely red and the flesh is soft [14]. So in practical tomato harvesting scenarios, the predominant method for assessing fruit ripeness involves non-destructive techniques such as machine vision [15–17], spectroscopy, hyperspectral imaging [18] and haptics. These methods are advantageous as they obviate the need for physical contact with the fruit. However, color-based imaging and spectroscopic technologies are significantly constrained by occlusion and illumination conditions, making them applicable only in stringent scenarios with complex equipment requirements. Conversely, acquiring information on fruit hardness through haptic during the harvesting process allows for direct ripeness determination, as hardness is a crucial factor determining fruit maturity [19]. While the color of the fruit may vary due to factors such as environmental temperature, hardness reflects changes in the internal starch content, providing a more accurate indication of internal tissue maturity [20]. The hardness of tomato undergoes significant changes during its developmental stages, decreasing by 30% as the fruit ripens [21]. Utilizing this information for the design of the harvesting strategy can improve the success rate of fruit harvesting. For instance, Luca Scimeca et al. [22] utilized a tactile sensor array mounted on a fruit harvesting device to capture tactile image sequences. Combining this with an elasticity-stiffness model, they determined the hardness of the mangoes and assessed their ripeness, achieved an accuracy of 88%. Jiahao Lin et al. [23] proposed a feasible strategy of estimating fruit hardness using soft claws and vision-based tactile perception, achieved an accuracy rate of 84.6%.

In this study, we proposed a method that utilizes a biomimetic gripper combined with flexible hydrogel sensors for tactile perception to estimate the ripeness of tomatoes. The design of the harvesting gripper is inspired by human-like fruit grasping behavior, featuring a three-fingered, six-jointed structure with fingers tailored to the curvature of the tomato. The integration of flexible hydrogel sensors serves to detect real-time gripping

forces during the fruit retrieval process, preventing damage to the fruit. The soft texture of the hydrogel material provides effective cushioning, achieving a compliant coupling effect when combined with the harvesting gripper. Furthermore, machine learning techniques are employed for real-time ripeness assessment. The approach involves transmitting force and deformation displacement data from each joint applied to the tomato during the harvesting process to a machine learning network. This method allows the tomato harvesting gripper to achieve damage-free picking while simultaneously providing immediate ripeness assessment during the harvesting process. This integrated approach reduces the need for subsequent labor-intensive sorting and classification operations, thereby significantly improving production efficiency.

Gel sensor

Material

Multi-walled carbon nanotubes (MWCNTs, outer diameter 5 ~ 15 nm, length 10 ~ 30 μm) were provided by Chengdu Organic Chemistry Co., Ltd., Chinese Academy of Sciences. In the laboratory, cellulose nanofibers with carboxylic acid groups on the surface (TOCNF, containing 0.89 mmol g^{-1}, diameter 20 ~ 50 nm, length ≥ 1 μm) were prepared through TEMPO oxidation. *N,N'*-Methylenebisacrylamide (MBA, 99%) and acrylamide (AM, 99%) were supplied by Shanghai Macklin Company. Ammonium persulfate (APS, 98%) was provided by Shanghai Aladdin Bio-Chem Technology Co., Ltd.

Preparation of hydrogel pressure sensors

Up to now, the conductive material system of flexible piezoresistive sensors is mainly made of carbon-based materials, such as carbon black (CBs) [24], carbon nanotubes (CNTs) [25], graphene nanoplatelets(GNPs) [26], nanowires(NWs), nanoparticles(NPs) [27], and their hybrid micro/nanostructures. Compared with metal materials, carbon-based fillers such as carbon fibers, carbon black, carbon nanotubes, and graphene have the advantages of high conductivity, low density, and high specific strength. Due to the advantageous properties of carbon-based hydrogels, the pressure sensor employs a carbon-based hydrogel as the sensing layer. Carbon-based conductive hydrogels exhibit outstanding comprehensive performance, presenting broad prospects for various applications [28, 29]. Among them, multi-walled carbon nanotubes (MWCNTs) have attracted significant attention due to its exceptional electrical, thermal, and mechanical properties. The high aspect ratio and surface-to-volume ratio make it particularly attractive for reinforcing polymers and hydrogels, thereby enhancing performance in a wide range of applications. Therefore, MWCNTs are chosen as the conductive material.

In this study, the hydrogel preparation process is illustrated in Fig. 1. Initially, 2.2670 g of TEMPO-oxidized cellulose nanofiber (TOCNF) gelatinous suspension, with a TOCNF content of 5.8%, was diluted by adding 12.0800 g of deionized water. The mixture was stirred to achieve a uniformly dispersed suspension. Subsequently, 0.0800 g of multi-walled carbon nanotubes (MWCNTs) was gradually added to the suspension, followed by magnetic stirring for 0.5 h to disperse the carbon nanotubes. Next, 5.5000 g (27.5 wt%) of acrylamide (AM) was added to the uniformly dispersed suspension, and magnetic stirring was conducted for an additional

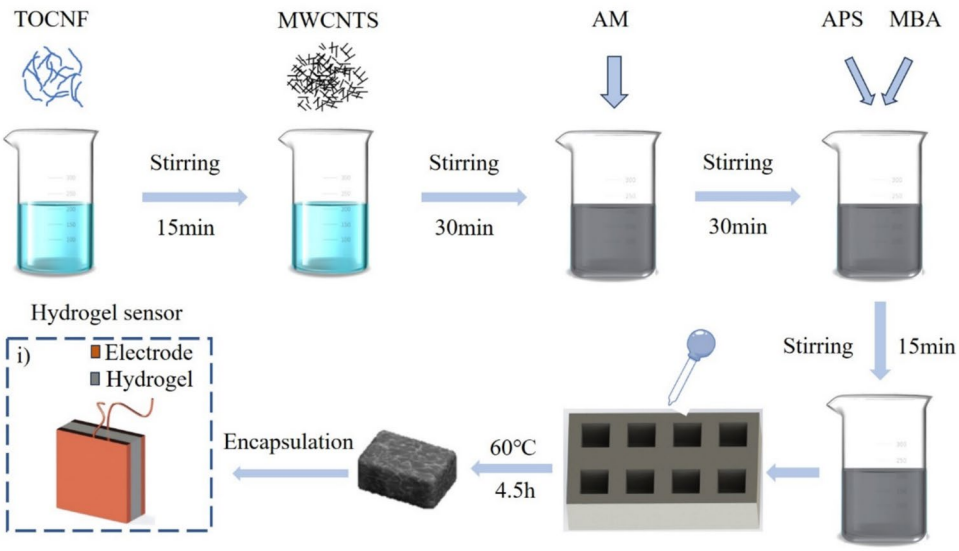

Fig. 1 The manufacturing process of the carbon-based hydrogel sensor, (i) Carbon-based hydrogel sensor

0.5 h. Subsequently, 0.110 g of ammonium persulfate (APS) and 0.0344 g of *N,N′*-methylenebisacrylamide (MBA) were introduced, and magnetic stirring continued for another 0.5 h to form the precursor solution for the hydrogel. The precursor solution was then injected into molds in an 8-well plate and cured by heating at a constant temperature of 50 °C for 4.5 h. This process resulted in the formation of the carbon-based conductive hydrogel. A pressure sensor was constructed using a sandwich-like structure, comprised the carbon-based hydrogel sensing layer, a polyimide (PI) film electrode, and a tape encapsulation layer. The schematic structure is depicted in Fig. 1(i).

Performance testing of the sensor

In order to demonstrate its potential applications, a comprehensive characterization of the resistive hydrogel pressure sensor was conducted, including mechanical performance, sensitivity, hysteresis, repeatability, stability, and detection range.

The mechanical and electrical properties of the hydrogel sensor were tested at room temperature. Compression tests were performed using a tensile testing machine (INSTRON 5565, America). In the mechanical performance characterization, hydrogel square samples with dimensions of 10×10×7 mm were subjected to a constant speed of 20 mm/min, and the pressure and strain were recorded. For electrical characterization, hydrogel samples with dimensions of 10×10×5 mm were encapsulated into sensor devices using the previously mentioned process. The relative change in resistance of the sensor devices was measured using an LCR digital bridge (TH2831, Tonghui, China). The relative resistance change rate was calculated using the following formula:

$$\Delta R/R_0 = \left(R - R_0\right)/R_0 \tag{1}$$

In this expression, R denotes the working resistance of the hydrogel sensor, and R_0 is the initial resistance before any applied pressure.

The sensor was placed on a tensile testing machine, a constant speed of 5 mm min^{-1} was set to characterize sensitivity and detection range by recording the resistance and pressure values during the compression process. To assess the response time of the sensor, a 10 g weight was placed on and then removed from the sensor, and the resistance curve under compression was recorded. Repeatability was evaluated through a loading–unloading cyclic test at 20% strain for 20 min using the tensile testing machine.

Flexible intelligent gripper

Gripper structure design

As has mimicked the human hand, the gripper of the tomato harvesting robot comprises three primary components: a motor driving the rotation of the gripper joints, a human-like gripper for tomato grasping, and a flexible sensor array for detecting the gripping force applied during tomato gripping. The motor that drives the joint rotation is furnished with a rotary encoder for the purpose of measuring the real-time angles at each joint. Utilizing the obtained angle data, the displacement at each point on the joint can be calculated, serving as the foundational for subsequent fruit ripeness detection. The tomato harvesting gripper is fabricated from resin material using 3D printing techniques, tailored to accommodate tomatoes with diameters ranging from 6 to 10 cm. Each joint surface of the picking fingers is intricately designed with small grooves for mounting gel-based pressure sensors, and the width of the finger structure is 30 mm. The gel sensors are securely affixed to the inner surface of the fingers using adhesive, as depicted in Fig. 2a. The flexible sensors provide soft contact and ensure accurate detection of gripping force during finger flexion, preventing damage to the tomatoes. The gripper structure is illustrated in Fig. 2b. As demonstrated in Fig. 2c, the operational sequence involves controlling the end effector to open the three fingers for tomato grasping, followed by closing the fingers securely around the tomato.

The research conducted by Jun Liu's team [12] on the physical properties of tomatoes indicates that, when selecting a finger structure with a width of 30 mm, the force applied to the tomato by a single finger should be less than 10 N. When the gel pressure sensors located on the inner side of the fingers detect a gripping force surpassing 10 N, the motor is then controlled to rotate the end effector, facilitating the smooth harvesting of the tomato without causing damage. This process contributes to the gentle and damage-free harvesting of tomatoes.

Intelligent harvesting solution

Tomatoes of the same variety were purchased from the Taobao online store "Maple Mountain Goods Pavilion".

Based on a carbon-based hydrogel sensor array, we proposed an intelligent system for flexible tomato harvesting and ripeness detection, as illustrated in Fig. 3. This harvesting solution primarily consists of a 3D-printed tomato harvesting gripper, a carbon-based hydrogel sensor array, a sensor data acquisition system, a signal processing

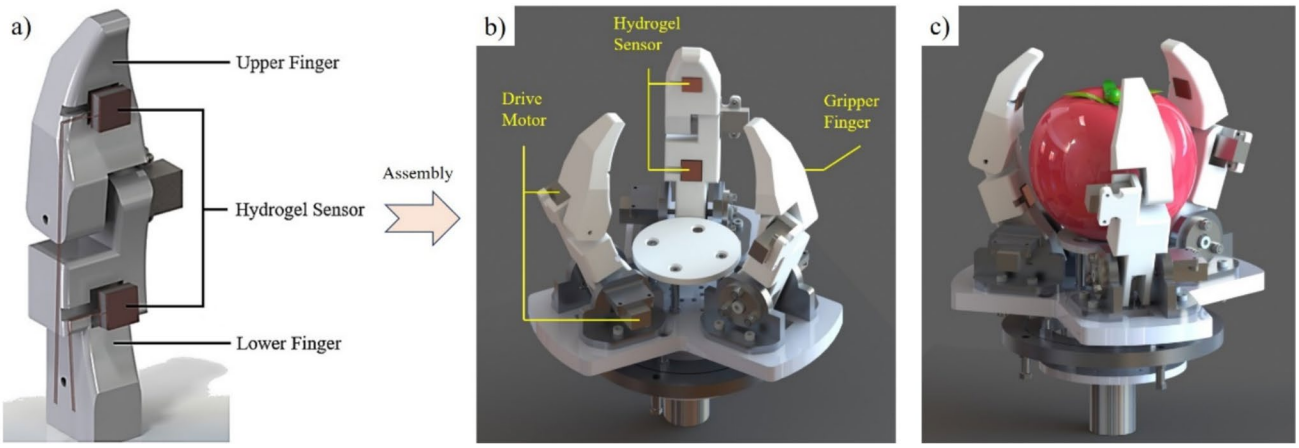

Fig. 2 Design and fabrication of tomato harvesting gripper. **a** Schematic design of finger, **b** three-finger gripper with sensors, **c** demonstration of gripper grasping a tomato

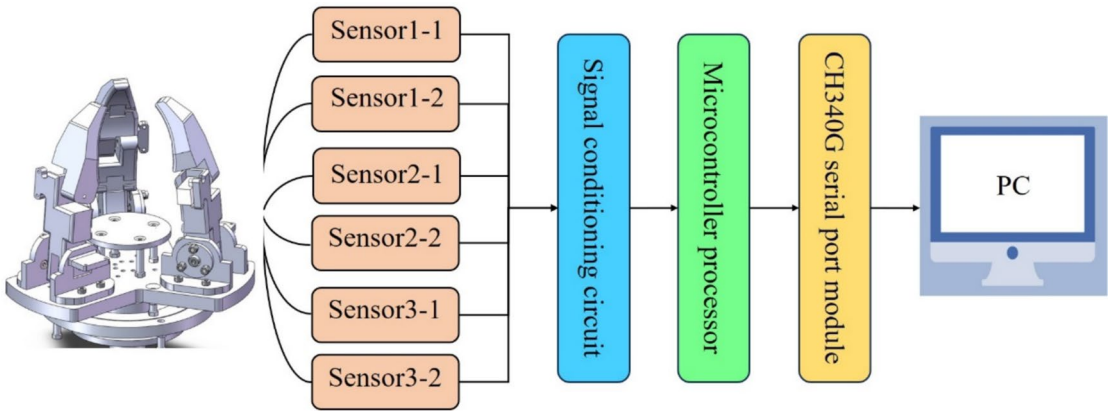

Fig. 3 Schematic diagram of flexible tomato harvesting and ripeness detection system

module, and a fruit ripeness detection system module. The 3D-printed gripper integrates six resistive pressure sensors to perceive the force applied at each finger joint during tomato harvesting, and it is integrated into the tomato-picking robot and controlled by the robot to grasp. The sensor data acquisition system connects to the hydrogel sensor array, measuring the electrical signals generated when the gripper grasps a tomato, then the electrical signals will be transmitted to the Microcontroller Processor. Subsequently, the electrical signal is converted into digital signal by the signal processing module integrated within the Microcontroller Processor. This digital signal then controls the flexible picking of tomatoes by the gripper. Finally, the processed data is transmitted to the PC. Thus, fruit ripeness detection is achieved based on machine learning technology. Finally, the upper-level interface promptly displays the grasping force and the estimated ripeness of the fruit.

Intelligent sensing system for harvesting process

With the rapid development of artificial intelligence technology, an increasing number of machinery and equipment are being integrated to comprehensively achieve intelligent decision-making, automatic control, and state recognition. By receiving data from various sensors installed on the equipment and utilizing machine learning to extract features of the equipment's operation under different conditions, advanced control can be implemented for the equipment [30–32]. Therefore, to design a harvesting gripper capable of both damage-free tomato picking and assessing fruit ripeness, machine learning are applied to feature extraction from the signals of the gel-based sensor array installed on the gripper and the motor's angular data during the tomato-grasping process. The signal acquisition module comprises the tomato harvesting gripper (Fig. 4a), a 6-channel sensor array signal conditioning module circuit board (Fig. 4b),

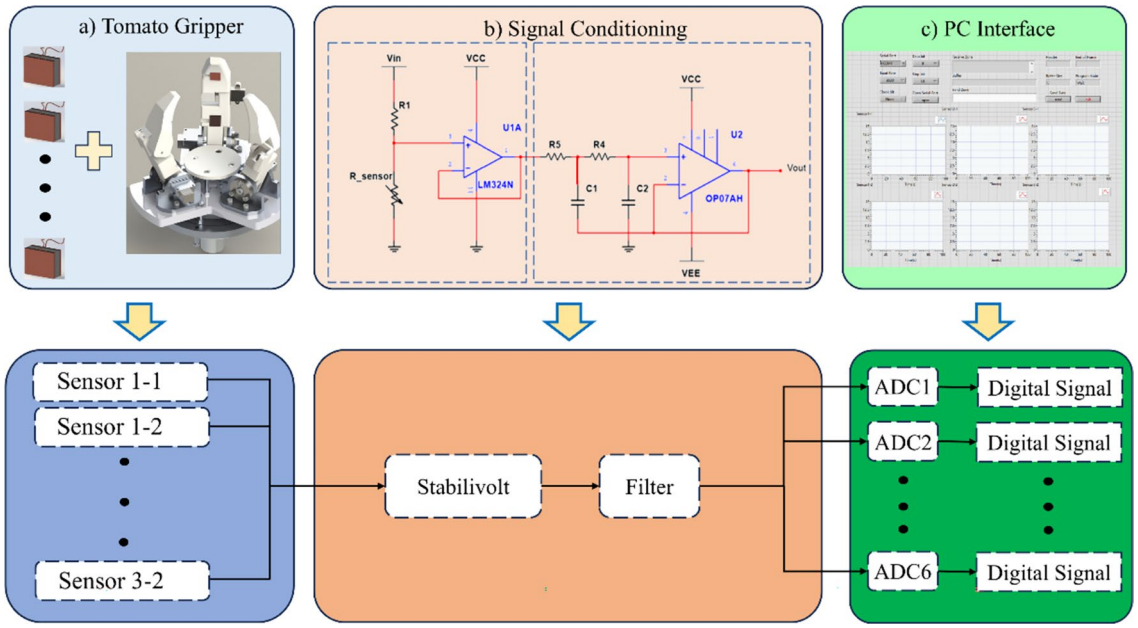

Fig. 4 Schematic Diagram of Tomato Flexible Harvesting Signal Acquisition Module. **a** Harvesting gripper, **b** circuit schematic of the sensor array signal conditioning module, **c** human–machine interaction interface

STC89C52 microcontroller, and LabVIEW host display interface (Fig. 4c).

The design of the signal conditioning and conversion circuit [33–35] for the resistive gel-based pressure sensor array is a crucial component of the automatic tomato harvesting system. The effectiveness of the circuit directly impacts the conversion of pressure signals. Following the principles of practicality, simplicity, and good performance, the circuit adheres to the design of the voltage divider circuit connected to the input of the voltage follower. The output of this circuit serves as the input to an active low-pass filtering circuit. In this circuit, R_{sensor} represents the resistance of the sensor. The output signal is calculated as follows:

$$V_{\text{out}} = V_{in}\frac{R_{sensor}}{R_{sensor} + R_1} \tag{2}$$

The data processed by the signal conditioning chip is further transmitted to the microcontroller. In the microcontroller, the median value average filtering method is utilized to filter the signals, ensuring the accuracy and reliability of the data. Based on the relationship between the resistance of the gel sensor and the applied pressure, the acquired resistance signals values are converted into pressure values. Through serial communication, the six-channel pressure data is transmitted to the LabVIEW display interface for visualization.

Simultaneously, the angular data of the motor controlling the gripper's movement is real-time recorded, with a frequency consistent with the sensor data acquisition module. When the gel-based sensor detects that the pressure has reached the critical force of 10 N for damage-free tomato gripping, the harvesting gripper ceases operation. Using the real-time angular data collected from the driving motor, the displacement of each joint-mounted sensor during the grasping process is calculated. The rotation angles of the finger joints' motors during the time period when the pressure values detected by the sensor increase from 0 N to the set value of 10 N are recorded. These rotation angle data, combined with the length of each joint of the gripper, can be used to calculate the deformation displacement caused by the force applied to the tomato during the harvesting process through geometric and physical derivation. The obtained data is saved as a dataset for future machine learning.

Tomato ripeness detection system

Figure 5a illustrates the algorithmic flowchart of the tomato ripeness detection system. The system collects data from the hydrogel pressure sensors and the motor angle sensors in the signal acquisition module. After processing the data to construct a dataset, an intelligent algorithm is needed to build a recognition model, ultimately achieving real-time identification and feedback. As the data collected in this experiment are the values of the force and deformation of tomatoes during the picking process, both of which have a causal relationship with the progression of time in the picking cycle, it belongs to the time series analysis and classification problem in machine learning tasks. And the most popular architectures and learning models include Long Short-Term Memory

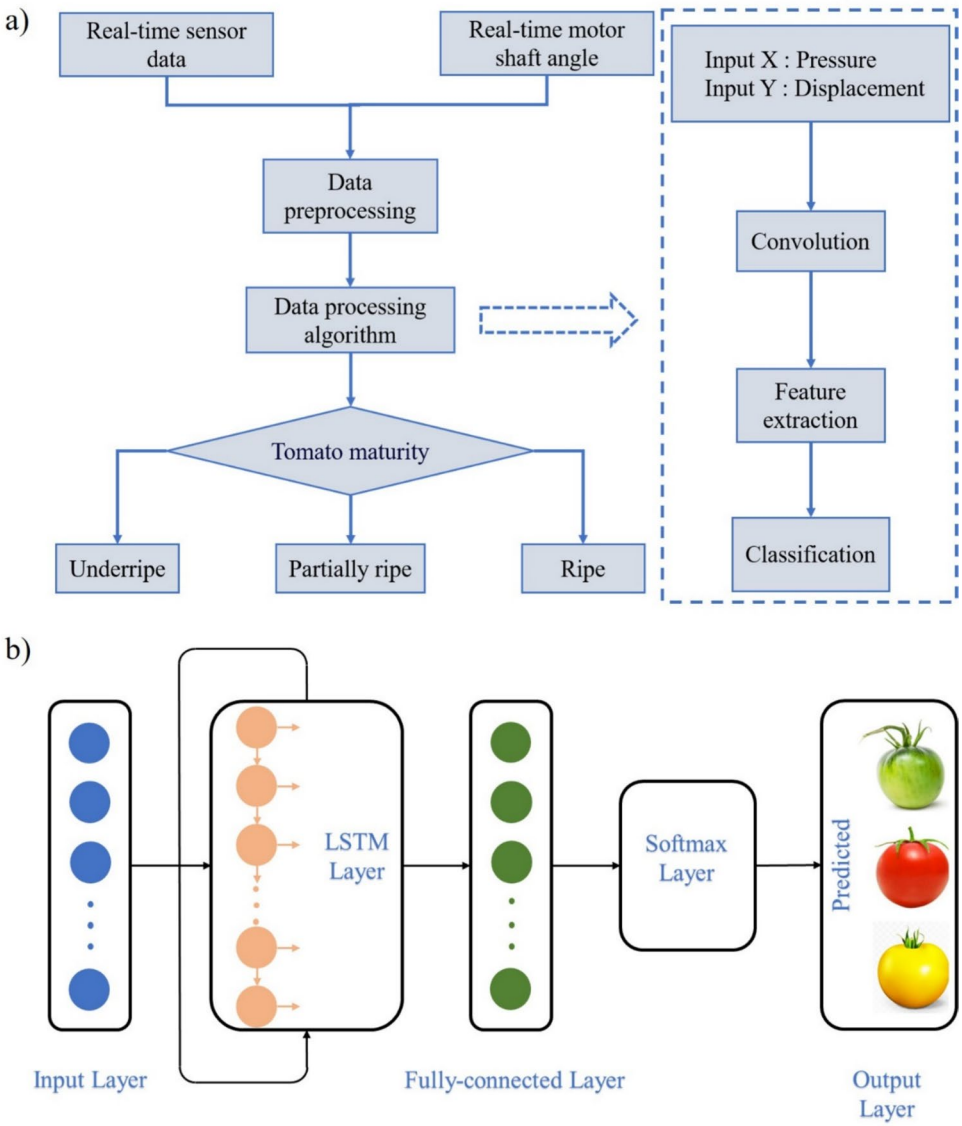

Fig. 5 Principles of the tomato ripeness detection system modules. **a** Flowchart of the fruit ripeness detection algorithm, **b** schematic diagram of the six-layer LSTM deep learning network architecture

(LSTM), Convolutional Networks (CNN), Multi-Layer Perceptron (MLP), and Fully Convolutional Networks (FCN). Among all studied models, the results show that long short-term memory (LSTM) and convolutional networks (CNN) are the best alternatives, with LSTMs obtaining the most accurate forecasts. CNNs achieve comparable performance with less variability of results under different parameter configurations, while also being more efficient [36].

To classify fruit ripeness based on the collected data, a five-layer Long Short-Term Memory (LSTM) network is employed for processing time-series sensor data. As a scheme comparison, the MLP, 1D-CNN, and FCN network structure are also employed to test the dataset. The design, training, validation, and testing of the LSTM network and other scheme comparison networks are implemented through the PyTorch deep learning toolbox. The architecture of the LSTM network is depicted in Fig. 5b. The input layer consists of six features corresponding to the 6-dimensional time-series sensor data from the six sensors on the end effector. The LSTM layer is designed with 180 hidden units, followed by a fully connected layer and employs the SoftMax activation function. The output layer provides three outputs corresponding to three different ripeness stages of the tomato fruit. And the MLP, 1D-CNN and FCN architecture are depicted in Figs. S1, S2, and S3 from, Supporting Information.

Results and discussion

Performance of flexible hydrogel pressure sensors

The compressive performance of the hydrogel was tested using a tensile testing machine, and the stress–strain curve

under compression is shown in Fig. 6a. Due to the reinforcing effect of MWCNFs on the hydrogel matrix, the prepared hydrogel exhibits good stress elasticity and strain elasticity. As shown in Fig. 6a, under pressure ranging from 0 to 100 kPa, the stress–strain curve of the hydrogel sample exhibits excellent linearity, precisely within the operational range of the pressure sensor used in this work. When conducting tests on the sensing characteristics of the hydrogel, two pieces of PI film electrodes were utilized to hold the conductive hydrogel in the middle, forming a sandwich structure. Two wires were connected to the PI film electrodes, and after the entire structure was assembled, it was

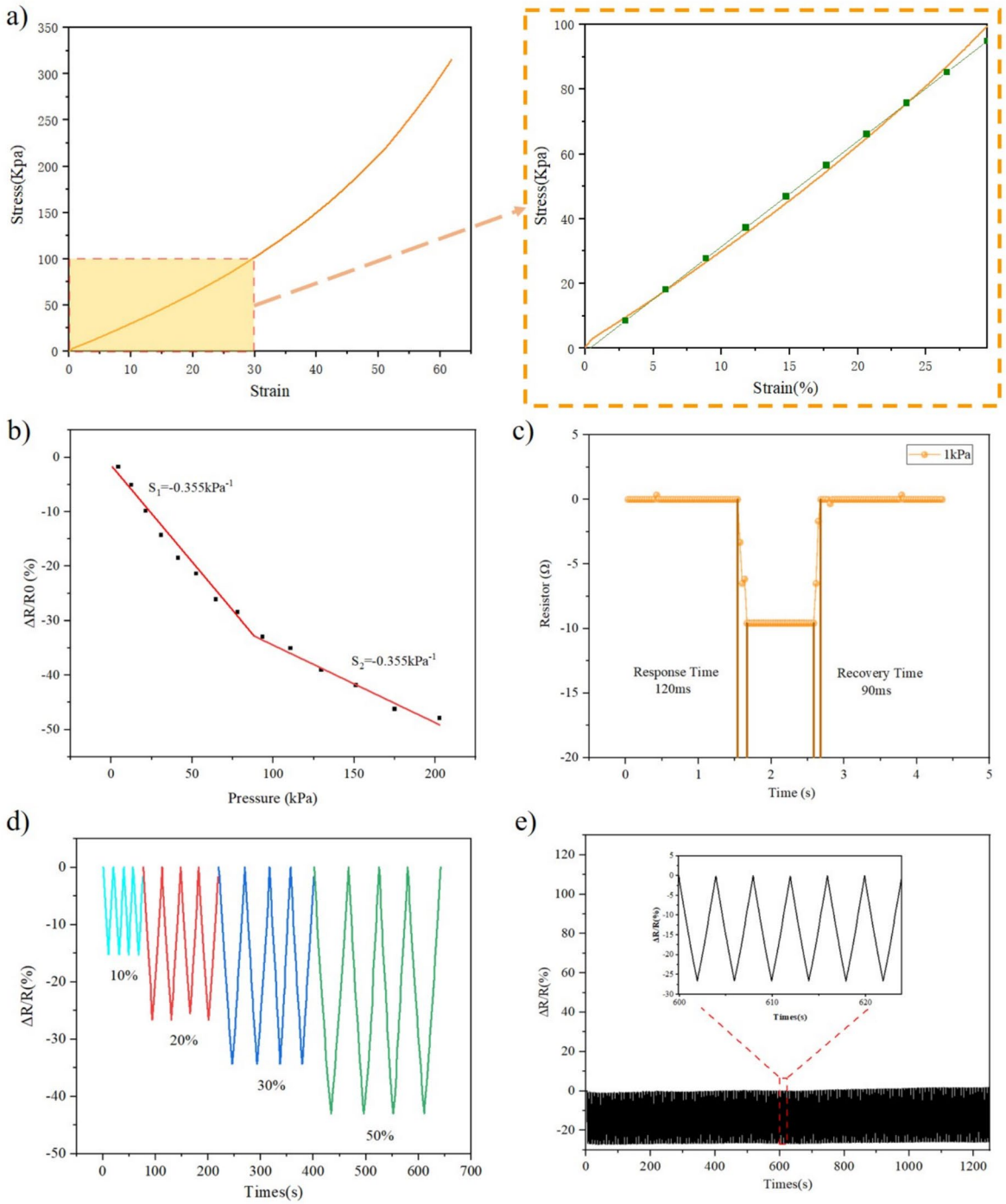

Fig. 6 Performance of hydrogel sensors. **a** Hydrogel stress–strain curve, **b** sensor sensitivity, c) Response time, **d** variation of relative resistance with compressive strain, e) Stability

sealed with tape, creating the sensing material. The response curve of the sensor is shown in Fig. 6b, indicating that the relative resistance value of the sensor steadily increases with the increase in stress, demonstrating good linearity. This enables the sensor to adapt well to the ability to detect force. As shown in Fig. 6c, under a stress of 1 kPa, the change in sensor resistance can be detected, with a response time of approximately 0.12 s during compression deformation and approximately 0.09 s for the sensor to return to its initial state under instantaneous stress release. This verifies the excellent response capability of the conductive gel.

Flexible sensors successfully detected compressive strains of 10, 20, 30, and 50% (Fig. 6d), demonstrating the hydrogel's outstanding sensing capability in terms of strain perception. After applying slight strain, the relative resistance significantly increased, proving its good sensitivity within the application range. Furthermore, the excellent strain compressibility of the material ensures structural connectivity or morphological integrity during compression, allowing the hydrogel sensor to generate clear and non-hysteric resistance signals under strain conditions.

Simultaneously, in-depth research was conducted on the fatigue resistance of the sensor. The sensor underwent a 20-min loading–unloading cycle under 20% strain on a tensile testing machine. The magnified insert in Fig. 6e illustrates the stability of the hydrogel electrical signal. During the loading–unloading process, there was a marginal increase in the $\Delta R/R_0$ value, likely associated with the disruption and reconstruction of chemical bonds within the conductive network. The results indicate that the sensor exhibits characteristics such as a broad detection range, high sensitivity, and excellent stability. These features make it well-suited for applications in detecting gripping forces during the tomato harvesting process.

Tomato ripeness detection based on machine learning

The varied signals collected during the harvest of tomatoes at different ripeness levels result from differences in the elastic modulus between tomatoes of different ripeness. Therefore, the compressed deformation values of fruits under a fixed pressure of 10 N applied by the gripper during the picking process also differ. Gripping experiments were conducted on ripe, semi-ripe, and unripe tomato samples in the experiment. The real-time output signals of processed tomatoes at different ripeness levels are shown in Fig. 7. Each curve represents the pressure and compressed displacement values experienced by the surface of the tomato that is in direct and close contact with the gel sensor installed on the gripper during the picking process. These values reflect the force applied to this particular surface of the tomato as

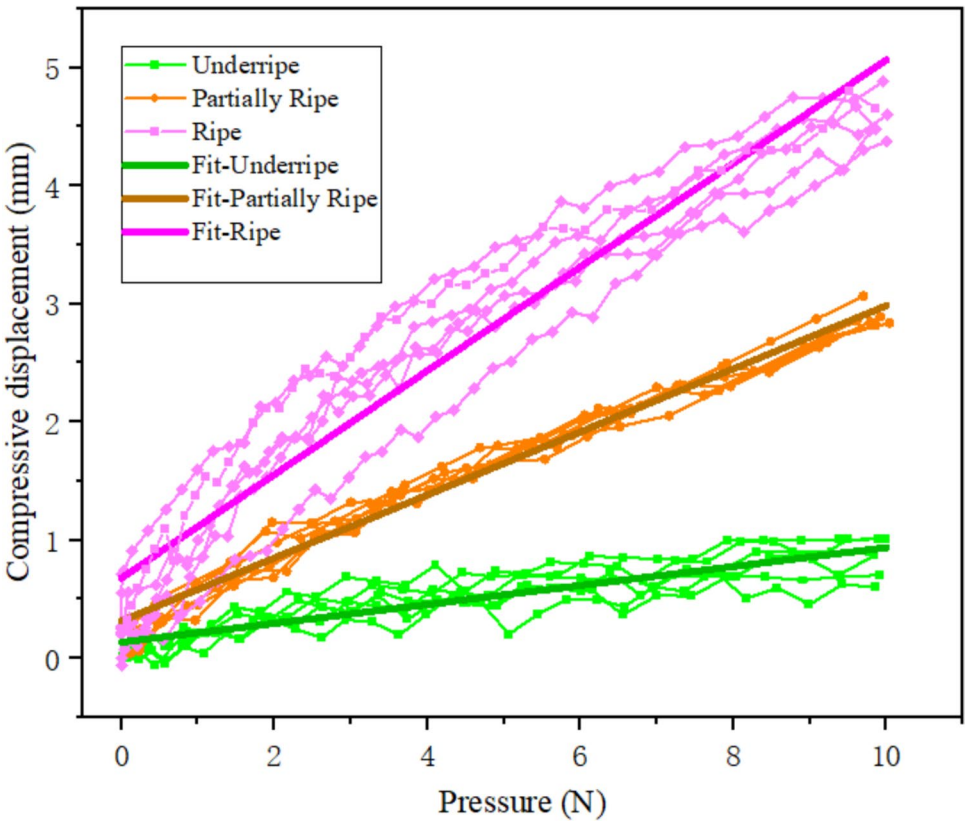

Fig. 7 Data Characterization of fruit ripeness detection based on tomato harvesting gripper (Corresponding to six-channel data curves for three different ripeness levels of tomatoes)

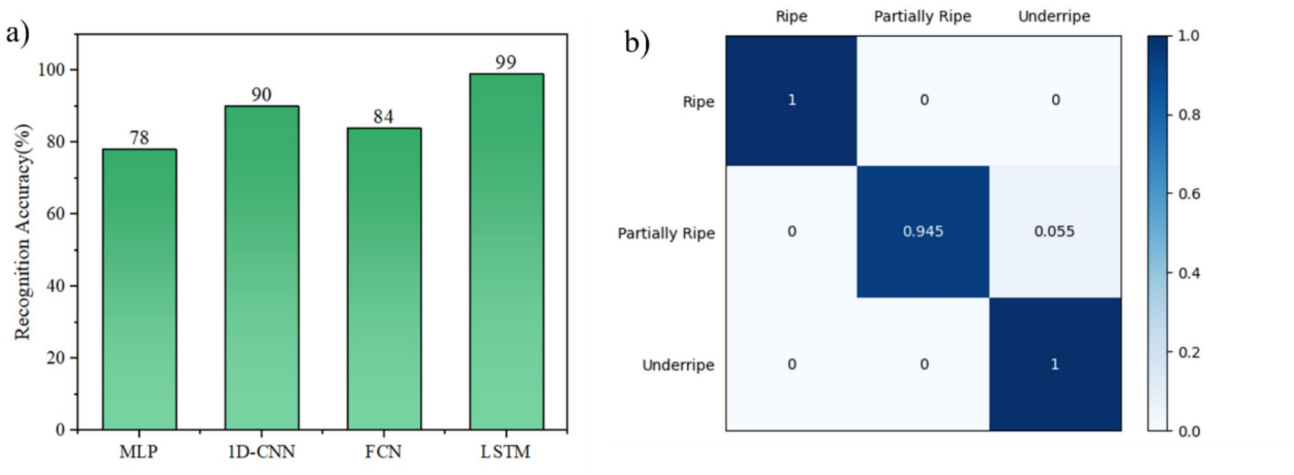

Fig. 8 Tomato Ripeness detection. **a** The average accuracy of the four constructed models in cross-validation, **b** confusion matrices using the LSTM network with fivefold validation scheme

it is being picked. It can be observed that the signals generated by tomatoes at different ripeness levels have distinct characteristics. Among them, ripe tomatoes exhibit the largest compressed displacement change during the gripping process, reaching an average deformation of 4.5 mm. Semi-ripe tomatoes follows, while unripe tomatoes show the smallest compressed displacement during gripping, a deformation of approximately 0.5 mm. Fitting the real-time output signals of the six sensors for the three ripeness levels of tomatoes reveals a clear difference in the slope of the signals generated during the gripping process. This is because the elastic modulus of ripe tomatoes is less than that of semi-ripe tomatoes, which, in turn, is less than that of unripe tomatoes. As a result, during the process in which the pressure applied by the gripper increases from 0 to 10 N, the signals gathered from tomatoes at different ripeness levels display distinct characteristics. This provides essential evidence for subsequent machine learning-based ripeness classification of fruits.

All the picking experiments during the data collection process were conducted under laboratory conditions. Before and after each tomato sample test, the integrity of the fruit was inspected to ensure that neither the skin nor the flesh was damaged. Only when these conditions were met was the data recorded as a valid sample. In the process of collecting training samples, each of the six sensors installed on the harvesting gripper recorded 450 data points for model training and recognition. A total of 100 tomatoes were collected as samples, comprising 51 unripe, 14 semi-ripe, and 35 ripe tomatoes. Classification performances were assessed by applying the fivefold cross validations on each of the 3 subjects's databases. In the fivefold cross-validation, the dataset is randomly divided into 5 subsets of equal size, and then each subset is tested using the classifier trained on the remaining 4 subsets. The network was trained using Adam Optimizer. Then, the obtained 5 classification accuracies were averaged to provide an overall classification accuracy. The accuracy of the four constructed models during cross-validation training is illustrated in Fig. 8a and Table S1, from Supporting Information. And one of the fivefold cross validation's loss function and accuracy function of the LSTM network are shown in Fig. S4 from, Supporting Information. It can be observed that the LSTM network exhibits the best performance, achieving an accuracy of 99%. The second-best is the 1D-CNN network, with an accuracy of 90%. The worst-performing model is the MLP, with an accuracy of only 78%. The confusion matrix based on the LSTM network is shown in Fig. 8b, revealing that only Partially ripe tomatoes are misclassified as Unripe, while the recognition accuracy for ripe tomatoes reaches 100%, which is precisely the desired outcome. These results demonstrate that the tomato harvesting gripper, equipped with the hydrogel pressure sensor, can utilize collected data and LSTM networks to achieve damage-free tomato harvesting and automatic estimation of fruit ripeness during the harvesting process.

Conclusion

This paper presents a rigid–flexible coupled harvest gripper that incorporates ionic hydrogel pressure sensors, enabling tomato ripeness detection through machine learning algorithms. First, a compressible and stable hydrogel was developed and integrated into sensors that are synchronized with the picking gripper, allowing for the measurement of finger bending angles and contact information during the tomato harvesting process. The use of flexible pressure sensors based on hydrogel ensures that tomato harvesting can

be conducted without causing damage to the fruit. A signal acquisition system was then designed to accurately collect data from the sensor array, capturing force signals during the tomato grasping operation. To analyze the sensor feedback data for tomato ripeness detection, four time series classification models were employed. The fivefold cross-validation results for 100 tomatoes with varying ripeness levels under ambient conditions demonstrated recognition accuracies of 78% (MLP), 80%(FCN), 90% (1D-CNN), and 99% (LSTM). These findings indicate that the LSTM network achieves the best classification performance. This study highlights that the gripper, equipped with hydrogel sensors, provides both flexible grasping capabilities and accurate estimation of tomato ripeness during robotic harvesting tasks. We expect to integrate the developed ripeness detection manipulation system on a mobile robot and to use it for fruit collection in the field. Future picking procedures will combine observation and motion to increase grasping success rate and to address other issues like designing appropriate control algorithms for detaching fruits from robust stems.

Supplementary Information The online version contains supplementary material available at https://doi.org/10.1007/s11694-025-03168-y.

Acknowledgements The authors gratefully acknowledge the financial support from the China Postdoctoral Science Foundation (No. 2023M731131) and the Guangdong Basic and Applied Basic Research Foundation (Nos. 2023A1515012023, 2023A1515110338).

Declarations

Conflict of interest The authors declare that they have none conflict of interest.

Replication of results Some or all data, models, or code generated or used during the study are available from the corresponding author by reasonable request.

References

1. Nations, F. a. A. O. o. t. U, Production/Crops and livestock products—Metadata. https://www.fao.org/faostat/en/#data/QCL/metadata
2. R.C. Ray, A.F. El Sheikha, S.H. Panda, D. Montet, Anti-oxidant properties and other functional attributes of tomato: an overview. Int. J. Food Ferment. Technol. **1**, 139–148 (2011)
3. Q. Vu, A. Ronzhin, Models and algorithms for design robotic gripper for agricultural products. Comptes Rendus De L Acad. Bulg. Des Sci. **73**, 103–110 (2020). https://doi.org/10.7546/crabs.2020.01.13
4. S. Vallone et al., An integrated approach for flavour quality evaluation in muskmelon (*Cucumis melo* L. *reticulatus* group) during ripening. Food Chem **139**, 171–183 (2013). https://doi.org/10.1016/j.foodchem.2012.12.042
5. E. Vrochidou et al., An overview of end effectors in agricultural robotic harvesting systems. Agric-Basel **12** (2022). https://doi.org/10.3390/agriculture12081240
6. Z. Wang, Y. Xun, Y. Wang, Q. Yang, Review of smart robots for fruit and vegetable picking in agriculture. Int. J. Agric. Biol. Eng. **15**, 33–54 (2022). https://doi.org/10.25165/j.ijabe.20221501.7232
7. Z. Li, X. Yuan, C. Wang, A review on structural development and recognition-localization methods for end-effector of fruit-vegetable picking robots. Int. J. Adv. Robot. Syst.**19** (2022). https://doi.org/10.1177/17298806221104906
8. C.-H Liu et al., In *IEEE/ASME International Conference on Advanced Intelligent Mechatronics (AIM).* pp. 92–97 (2019).
9. T. Fujinaga, S. Yasukawa, K. Ishii, In *IEEE/SICE International Symposium on System Integration (SII).*.IEEE, pp 628–633 (2021).
10. H. Zhou et al., Learning-Based Slip Detection for robotic fruit grasping and manipulation under leaf interference. Sensors **22** (2022). https://doi.org/10.3390/s22155483
11. F. Zhang et al., Research on flexible end-effectors with humanoid grasp function for small spherical fruit picking. Agric.-Basel **13** (2023). https://doi.org/10.3390/agriculture13010123
12. Y. Zheng, et al., Design and simulation of a gripper structure of cluster tomato based on manual picking behavior. Front. Plant Sci. **13** (2022). https://doi.org/10.3389/fpls.2022.974456
13. L. Li, W. Tian, Z. OuYang, S. Yu, W. Sun, In *40th Chinese Control Conference (CCC).*, pp 4068–4072 (2021).
14. H.-L. Zhang et al., Effects of harvest ripeness on storage quality of tomato fruits. Emirates J. Food Agric. **35**, 978–987 (2023). https://doi.org/10.9755/ejfa.2023.v35.i11.3166
15. E. Bonah, X. Huang, J.H. Aheto, R. Osae, Application of hyperspectral imaging as a nondestructive technique for foodborne pathogen detection and characterization. Foodborne Pathog. Dis. **16**, 712–722 (2019). https://doi.org/10.1089/fpd.2018.2617
16. T. Kim, D.-H. Lee, K.-C. Kim,, T. Choi, J.M. Yu, Tomato maturity estimation using deep neural network. Appl. Sci.-Basel **13** (2023). https://doi.org/10.3390/app13010412
17. A. Khan et al., Tomato maturity recognition with convolutional transformers. Sci. Rep. **13**, 22885–22885 (2023). https://doi.org/10.1038/s41598-023-50129-w
18. A. Torregrosa, E. Orti, B. Martin, J. Gil, C. Ortiz, Mechanical harvesting of oranges and mandarins in Spain. Biosys. Eng. **104**, 18–24 (2009). https://doi.org/10.1016/j.biosystemseng.2009.06.005
19. Overview of the methods for assessing harvest maturity, Stewart Postharvest Rev. **8**, 1–11 (2012). https://doi.org/10.2212/spr.2012.1.4
20. L.-s. Zhu, et al. Ethylene-induced banana starch degradation mediated by an ethylene signaling component MaEIL2. Postharvest Biol. Technol. **181** (2021). https://doi.org/10.1016/j.postharvbio.2021.111648
21. M.M. Alenazi, et al. Non-destructive assessment of flesh firmness and dietary antioxidants of greenhouse-grown tomato (*Solanum lycopersicum* L.) at different fruit maturity stages. Saudi J. Biol. Sci. **27**, 2839–2846 (2020). https://doi.org/10.1016/j.sjbs.2020.07.004
22. L. Scimeca, et al. in *IEEE international conference on robotics and automation (ICRA).*, pp 1821–1826 (2019).
23. Chen, Y. et al. in *IEEE International Conference on Robotics and Automation (ICRA).* pp 2303–2309 (2022).
24. D. Yu et al., Multi-responsive and conductive bilayer hydrogel and its application in flexible devices. RSC Adv. **12**, 7898–7905 (2022). https://doi.org/10.1039/d1ra09232d
25. Z. Qin et al., Carbon Nanotubes/hydrophobically associated hydrogels as ultrastretchable, highly sensitive, stable strain, and pressure sensors. ACS Appl. Mater. Interfaces. **12**, 4944–4953 (2020). https://doi.org/10.1021/acsami.9b21659
26. J.P. Chamberland, A. J. Sellathurai, J.S. Parent, D. P. J. Barz, Optimized hydrogel electrodes for supercapacitors from high-concentration aqueous graphene nanoplatelet dispersions. J.

Power Sources **605** (2024). https://doi.org/10.1016/j.jpowsour.2024.234435
27. N. Wen et al., Overview of polyvinyl alcohol nanocomposite hydrogels for electro-skin, actuator, supercapacitor and fuel cell. Chem. Rec. **20**, 773–792 (2020). https://doi.org/10.1002/tcr.202000001
28. W. Zhang, X. Zhang, W. Zhao, X. Wang, High-sensitivity composite dual-network hydrogel strain sensor and its application in intelligent recognition and motion monitoring. Acs Appl. Polymer Mater. **5**, 2628–2638 (2023). https://doi.org/10.1021/acsapm.2c02215
29. Z. Guo et al. Multifunctional flexible polyvinyl alcohol nanocomposite hydrogel for stress and strain sensor. J. Nanoparticle Res. **23** (2021). https://doi.org/10.1007/s11051-021-05333-y
30. W.-X. Lu et al., Artificial intelligence-enabled gesture-language-recognition feedback system using strain-sensor-arrays-based smart glove. Adv. Intell. Syst. (2023). https://doi.org/10.1002/aisy.202200453
31. R. Zuo et al., in *IEEE International Conference on Robotics and Automation (ICRA)*. pp 12164–12169 (2021).
32. Q. Li et al., Ultrastretchable high-conductivity MXene-based organohydrogels for human health monitoring and machine-learning-assisted recognition. ACS Appl. Mater. Interfaces. **15**, 19435–19446 (2023). https://doi.org/10.1021/acsami.3c00432
33. J. Liu, Y. Zhang, Y. Lu, S. Ren, S. Cao, Augmented nested arrays with enhanced DOF and reduced mutual coupling. IEEE Trans. Signal Process. **65**, 5549–5563 (2017). https://doi.org/10.1109/tsp.2017.2736493
34. Q.-B. Zhu et al., A flexible ultrasensitive optoelectronic sensor array for neuromorphic vision systems. Nature Commun. **12** (2021). https://doi.org/10.1038/s41467-021-22047-w
35. C.-L. Liu, P.P. Vaidyanathan, Super nested arrays: linear sparse arrays with reduced mutual coupling-Part I: fundamentals. IEEE Trans. Signal Process. **64**, 3997–4012 (2016). https://doi.org/10.1109/tsp.2016.2558159
36. P. Lara-Benitez, M. Carranza-Garcia, J. C. Riquelme, An experimental review on deep learning architectures for time series forecasting. Int. J. Neural Syst. **31** (2021). https://doi.org/10.1142/s0129065721300011